CATARACT SURGERY

Femtosecond Laser–Assisted Cataract Surgery with Integrated Optical Coherence Tomography

Daniel V. Palanker,[1]* Mark S. Blumenkranz,[1] Dan Andersen,[2] Michael Wiltberger,[2] George Marcellino,[2] Phillip Gooding,[2] David Angeley,[2] Georg Schuele,[2] Bruce Woodley,[2] Michael Simoneau,[2] Neil J. Friedman,[1] Barry Seibel,[3] Juan Batlle,[4] Rafael Feliz,[4] Jonathan Talamo,[5] William Culbertson[6]

(Published 17 November 2010; Volume 2 Issue 58 58ra85)

About one-third of people in the developed world will undergo cataract surgery in their lifetime. Although marked improvements in surgical technique have occurred since the development of the current approach to lens replacement in the late 1960s and early 1970s, some critical steps of the procedure can still only be executed with limited precision. Current practice requires manual formation of an opening in the anterior lens capsule, fragmentation and evacuation of the lens tissue with an ultrasound probe, and implantation of a plastic intraocular lens into the remaining capsular bag. The size, shape, and position of the anterior capsular opening (one of the most critical steps in the procedure) are controlled by freehand pulling and tearing of the capsular tissue. Here, we report a technique that improves the precision and reproducibility of cataract surgery by performing anterior capsulotomy, lens segmentation, and corneal incisions with a femtosecond laser. The placement of the cuts was determined by imaging the anterior segment of the eye with integrated optical coherence tomography. Femtosecond laser produced continuous anterior capsular incisions, which were twice as strong and more than five times as precise in size and shape than manual capsulorhexis. Lens segmentation and softening simplified its emulsification and removal, decreasing the perceived cataract hardness by two grades. Three-dimensional cutting of the cornea guided by diagnostic imaging creates multiplanar self-sealing incisions and allows exact placement of the limbal relaxing incisions, potentially increasing the safety and performance of cataract surgery.

INTRODUCTION

Cataract surgery is the most frequently performed surgical procedure in the United States, with more than 1.5 million procedures each year (*1*). It is estimated that about one-third of Americans will undergo cataract surgery in their lifetime. Currently, the procedure begins with a small corneal incision to allow manual formation of an opening in the anterior lens capsule (capsulorhexis), followed by ultrasound-assisted emulsification and removal of the opacified crystalline lens (phacoemulsification), and subsequent insertion of a synthetic intraocular lens (IOL). Although this manual procedure is generally regarded as safe and effective, its outcome depends heavily on the skills and experience of the surgeon. Potentially serious complications may occur, including injury to the cornea, iris, anterior and posterior lens capsules, inadvertent subluxation of lenticular fragments, and vitreous loss, which may significantly degrade patient's vision.

The capsulorhexis, or continuous curvilinear capsulotomy, provides the surgeon access to the lens for its removal with the phacoemulsification probe, as well as a route for delivery of the IOL into the capsular bag. It is a critical step in cataract surgery. A properly sized, shaped, and centered capsulorhexis enhances surgical safety, hydrodissection of the lens, nuclear disassembly and removal, cleanup of the remaining cortex, and IOL centration, and inhibits posterior capsular opacification (*2*–*11*). The advent of newer refractive IOLs (accommodating, multifocal, and aspherical designs) has further elevated the importance of consistently achieving a symmetrically round and properly sized and placed capsulorhexis, because centration of the IOL depends on these features (*12*). Misalignment of the IOL, especially a multifocal one, which can occur with suboptimal construction of the capsulorhexis, produces a number of bothersome or even disabling optical aberrations for the patient. For the novice surgeon, the capsulorhexis is usually rated as the single most difficult step in cataract surgery (*13*). Even for experienced surgeons, however, achieving a properly sized and centrally positioned capsulorhexis is more difficult in the presence of a variety of common surgical risk factors that include small pupils, a shallow anterior chamber, weak zonules, a pediatric eye, poor visibility, and lack of a red reflex. The capsulorhexis is one of the few surgical steps in cataract surgery that has not yet been enhanced by technology. The maneuver is still performed free hand, relying on visual clues such as the pupillary and corneal diameter, as estimated by the surgeon.

There are other sources of adverse events during cataract surgery. Excessive use of ultrasound energy during phacoemulsification of hard cataracts can result in damage to corneal endothelium and thermal injury to the cornea at the probe insertion site (*14*). In addition, the safety of mechanical manipulation of the lens during surgery is limited in cases of weak zonules (thin fibrils attaching the lens capsule to ciliary muscle). Suboptimal construction of the cataract incision may result in leakage, ocular hypotension (hypotony), iris prolapse, or intraocular infection. Cataract incisions created with microsurgical blades typically have a simple uniplanar configuration. Fluids may leak in and out of the eye through poorly constructed incisions with inadequate dimensions and orientation (*15*, *16*). As a result, bacteria in the tear film may enter the anterior chamber of the eye and cause a

[1]Department of Ophthalmology, Stanford University, Stanford, CA 94305, USA. [2]OptiMedica Corp., Santa Clara, CA 95054, USA. [3]Seibel Vision Surgery, Los Angeles, CA 90025, USA. [4]Laser Centro, Santo Domingo, Dominican Republic. [5]Talamo Laser Eye Consultants, Waltham, MA 02451, USA. [6]Bascom Palmer Eye Institute, Miami, FL 33136, USA.
*To whom correspondence should be addressed. E-mail: palanker@stanford.edu

vision-threatening intraocular infection. Complex multiplanar incision such as an interlocking zigzag or tongue-in-groove design could provide a more self-sealing configuration. Manually performed corneal relaxing incisions for correction of astigmatism may also suffer from imprecise depth, position, length, and shape of the cut.

Precise dissection of the cornea with femtosecond lasers advanced the exactitude and safety of refractive surgery [laser-assisted in situ keratomileusis (LASIK)] compared with the previous mechanical cutting of the corneal flap (*17*, *18*). Similar benefits could be provided for cataract surgery if laser patterns could be properly aligned across the target tissues. We developed a system that combines optical coherence tomography (OCT) for three-dimensional mapping of the eye, with a femtosecond pattern scanning laser for capsulotomy, lens segmentation, and fragmentation, as well as for the corneal incisions.

RESULTS

Preclinical results

We first assessed the quality of lens capsule cutting by the femtosecond laser using freshly enucleated porcine eyes. The crystalline lens was extracted from the eye and placed in a container with balanced salt solution (BSS) and covered with a thin (#1) coverslip. The lens was placed horizontally, with the anterior part facing up. The laser beam was directed into the tissue vertically from above through the cover slip. A spiral laser pattern was applied to the anterior lens capsule starting from 200 μm under the anterior capsule and ending 200 μm above it. Using ~100 samples, we determined the threshold energy and pattern spot density required to produce a continuous cut. With a pulse duration of ~400 fs, a wavelength of 1.03 μm, and a focal spot size <10 μm, the required threshold pulse energy was ~3 μJ, although actual cutting required higher energies. To produce a continuous cut of the lens capsule, we found the lateral spot spacing (in the anterior plane of the tissue) to be ~5 μm, with an axial (or depth) spacing of 10 μm. For lens segmentation, lateral spacing (in a horizontal plane) could be increased to 10 μm with an axial spacing of 20 μm. An example of a cut in a porcine capsule is shown in Fig. 1. Residual bubbles of about 40 to 70 μm in diameter become trapped between the edges of the cut, as seen in the image.

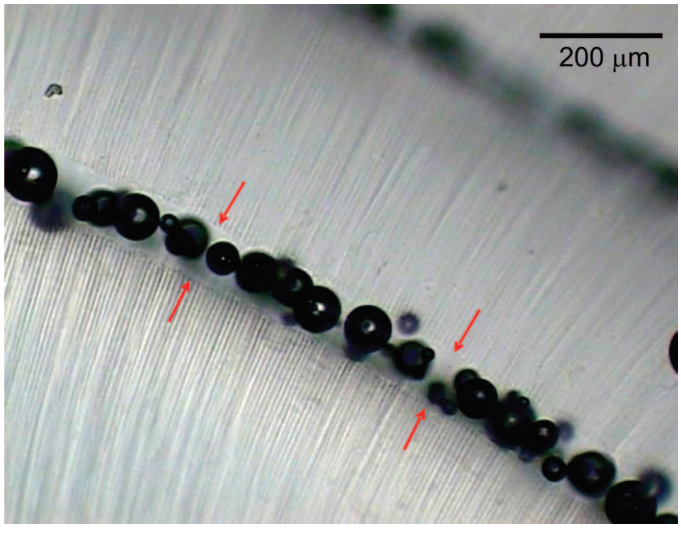

Fig. 1. Image of a cut in a porcine lens made with a femtosecond laser. Capsule of a porcine lens cut in vitro at the following pulse parameters: 10 μJ per pulse, 50 kHz, 4 μm per step. The sharp edges of the cut capsule (arrows) separate after dissection, trapping residual gas bubbles in the gap.

We next tested the strength of the cut capsular edge in porcine eyes. A specialized instrument including motorized translation stages was built to stretch the tissue at a constant rate. Semicircular pins with radius of curvature of 2 mm were inserted into the 4.6-mm-diameter capsulotomy opening and pulled symmetrically in opposite directions until the capsule ruptured. The applied force was registered by piezoelectric dynamometers on both sides and recorded. Twelve laser-treated eyes and 12 eyes with manual capsulorhexis performed by an experienced cataract surgeon (N.J.F.) were studied. The average strength of the capsule after manual capsulorhexis was 66 (±22 SD) mN; after laser capsulotomy, it was more than twice as high: 152 (±21 SD) mN. A stronger capsulotomy could help to reduce the probability of inadvertent rupture of the capsule during lens emulsification and insertion of the IOL.

Additional testing was performed on enucleated human eyes (100 samples). For better lens preservation in these eyes, only the cornea and iris were removed to allow cutting of the lens in an otherwise whole eye. As with the porcine samples, human eyes were submerged in BSS and covered with a thin coverslip. Scanning laser parameters for segmentation of the lens capsule and the lens cortex were found to be similar to those used in porcine samples: a threshold pulse energy of 3 μJ, lateral spot spacing of 5 μm, and axial spacing of 10 μm for capsulotomy, and twice that size for lens segmentation.

In vivo retinal safety assessment

We tested the potential damage to the retina as a result of laser exposure using six Dutch belted rabbits (12 eyes) in vivo. To test the worst-case scenario, we applied the maximum settings of the laser (6 μJ, 100 kHz) without any scanning for up to 60 s in each eye. In addition, to avoid beam attenuation on plasma and gas bubbles, the beam was slightly defocused to prevent dielectric breakdown while maintaining the same retinal beam diameter. We then examined the retina with fluorescein angiography and ophthalmoscopic imaging within 1 hour of irradiation, and again 3 days later. With the irradiation exposures we tested, no retinal or other ocular damage was observed (fig. S1).

System design for human surgery

To apply laser cutting to the anterior crystalline lens capsule and nucleus in clinical practice, the system should ensure the safety and integrity of all the tissues nearby, such as posterior corneal surface, iris, and posterior lens capsule. Therefore, proper sizing and positioning of the dissection patterns for each patient must be based on an accurate map of the eye's anterior segment. To ensure stable positioning during laser surgery, the eye is docked to the optical system via a contact lens with a concave surface proximal to the anterior cornea (Fig. 2). This contact lens includes a circumferential suction skirt, as in femtosecond refractive laser systems. To minimize eye deformation, the curvature of the concave surface on the contact lens closely matches the native corneal shape. However, because corneal curvature varies among patients, the eye is partially deformed from its native shape, and thus the OCT mapping must be performed after docking to ensure accuracy. Therefore, we developed a long-range,

frequency-domain OCT (FDOCT) imaging system, which is integrated with the femtosecond laser optics and applied through the common focusing objective and the contact lens (fig. S2). This system has an axial resolution of ~11 μm, allowing for precise detection of the cornea, iris, and both anterior and posterior lens surfaces.

The three-dimensional map of the lens and the anterior chamber is acquired with FDOCT, and the software automatically identifies the anterior and posterior surfaces of the lens and cornea, as well as the iris (Fig. 3A). On the basis of the OCT image, and taking into account predefined safety margins to prevent inadvertent injury to the cornea, iris, or posterior lens capsule, the software overlays the prospective capsulotomy and the lens segmentation patterns onto the OCT data for the physician's review on a graphical user interface (GUI) (Fig. 3A). OCT imaging also allows for exact positioning of the corneal relaxing incisions and multiplanar self-sealing cataract incision. Because laser cutting is performed before introduction of the patient into the sterile environment of the operating room, the cataract incision does not penetrate the posterior corneal surface.

In addition to OCT, the system provides a live en face view of the eye via a video camera operating through the same objective and contact lens (Fig. 3B). Boundaries of the planned capsulotomy and lens segmentation patterns are overlaid on the live image, allowing the physician to verify the placement of the patterns and to adjust them, if needed. Examples of the scanning patterns for capsulotomy, lens segmentation, and fragmentation are shown in Fig. 3C. Three-dimensional rendering of the capsulotomy and segmentation patterns in the lens is shown in Fig. 3D.

On the basis of the preclinical experiments described above, we selected the following range of parameters for operation of the femtosecond laser system: pulse duration of ~400 fs, wavelength of 1.03 μm, focal spot size <10 μm, pulse energy range of 3 to 10 μJ, and pulse repetition range of 12 to 80 kHz; scanning parameters: lateral spot spacing of about 5 μm for capsulotomy and 10 μm for lens segmentation; axial spacing: about 10 μm for capsulotomy and 20 μm for lens segmentation.

Clinical results

We performed cataract surgery on a total of 50 patients. After the patient was docked to the system and OCT was performed, the physician selected the surgical patterns and adjusted the laser parameters, if necessary. First, a spiral capsulotomy pattern was applied from posterior

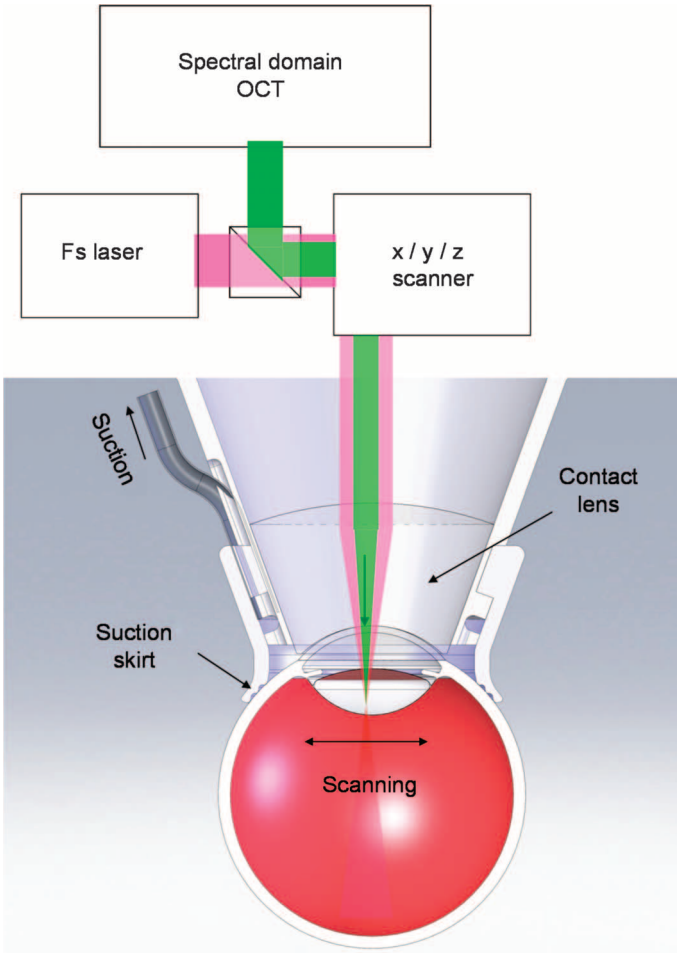

Fig. 2. Diagram of the optical and mechanical interface between the laser system and the eye. The femtosecond (Fs) laser and OCT beam share the same optical path, providing an exact co-registration of the OCT image with the laser segmentation patterns. OCT, optical coherence tomography.

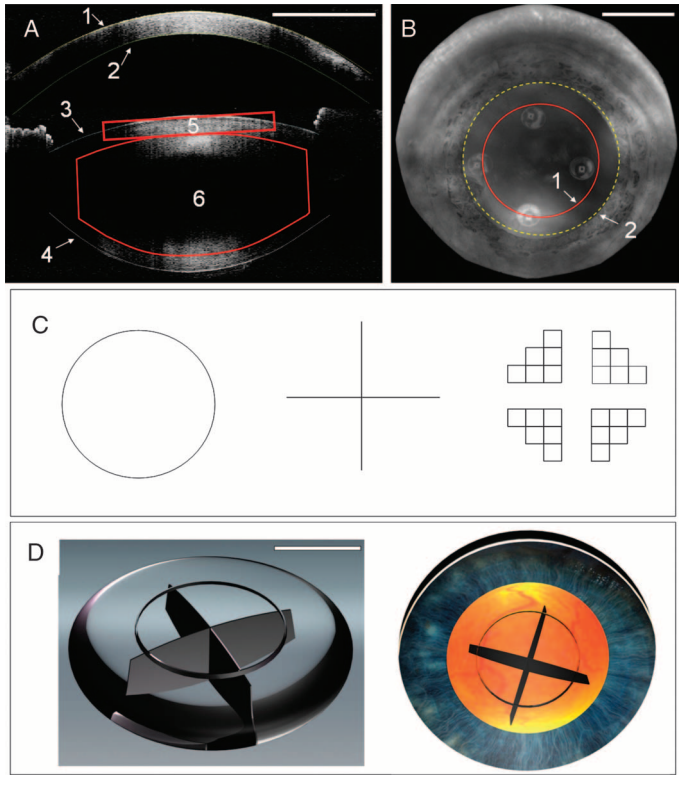

Fig. 3. Images and cutting patterns produced by the system. (**A**) OCT image of the eye with outlined boundaries of the cornea (1 and 2) and lens capsule (3 and 4). The capsulotomy pattern (5) and lens segmentation pattern (6) are shown in solid red. (**B**) View of the eye via the near-infrared video camera, with overlaid guidance lines indicating a planned capsulotomy pattern (1) and a boundary of the pupil (2). (**C**) Top view of the circular capsulotomy pattern, a cross-pattern for lens segmentation, and the nucleus fragmentation pattern. (**D**) Three-dimensional representation of the capsulotomy and cross-segmentation patterns in the lens alone (left) and inside the eye (right). Scale bars, 3 mm.

to anterior, thereby ensuring intersection of the incision with the anterior lens capsule in between. This upward propagation avoided scattering of the laser beam before its focal point on the microbubbles that form in previously treated locations. In addition, the bubbles formed in the depth of tissue below the current laser focus scatter the laser beam propagating beyond the focal spot, thus helping to reduce the amount of laser radiation reaching the retina. The capsulotomy pattern was applied before lens fragmentation because a significant number of gas bubbles formed during lens fragmentation, when a large number of pulses are applied, could stretch and displace the lens capsule from its original position, causing the relatively shallow capsulotomy laser pattern to miss the capsule. On the other hand, the relatively small number of bubbles formed during capsulotomy did not appreciably affect the position of the lens, and thus, alignment of the lens segmentation and fragmentation patterns remained sufficiently precise. The circular pattern produced by the laser capsulotomy is shown in Fig. 4A (see also video S1).

After the capsulotomy step was completed, the lens segmentation and fragmentation patterns were applied, again starting from the posterior part of the lens and propagating anteriorly. Gas generated inside the lens made it more reflective and the laser pattern more visible in the integrated video system (Fig. 4B). In addition to the vertical laser cuts, gas formed during the lens fragmentation helped to separate the horizontal lens lamella, which further enhanced its softening (pneumodissection) (see video S2). Slight expansion of the lens as a result of gas formation sometimes led to lifting of the capsulotomy disk.

In contrast to manual cataract surgery, in which the corneal incision is performed first, laser cutting of the cornea was the last step. The pattern for the corneal entry incision was constructed of three planes (Fig. 5). The offset of the incision formed a one-way valve that was self-sealing and water tight under physiological intraocular pressure. The laser scanning began ~200 μm anterior to the posterior surface of the stroma and propagated all the way to its external surface. In this way, the procedure could be performed outside of the operating room because the incision was not complete, and therefore the integrity of the anterior chamber was not violated prior to the patient entering the operating suite and undergoing sterile prepping and draping. The final internal 200 μm was penetrated in the operating room by inserting a microsurgical blade into the anterior chamber through the partial thickness laser incision. Such a multiplanar incision is demonstrated in a postsurgical OCT image in Fig. 5B.

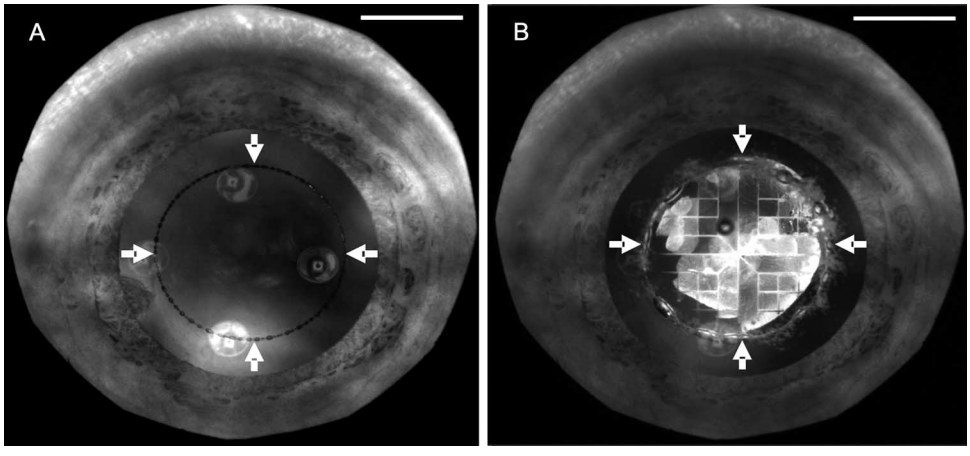

Fig. 4. Images of the eye after cuts are made. (**A**) View of the eye via the near-infrared video camera after the laser capsulotomy. Arrows, bubble-filled circular line of the laser cut. (**B**) A view of the eye after the lens segmentation and fragmentation. Lens becomes much brighter due to enhanced light scattering by the gas bubbles. Arrows, bubble-filled circular line of the laser cut. Scale bars, 3 mm.

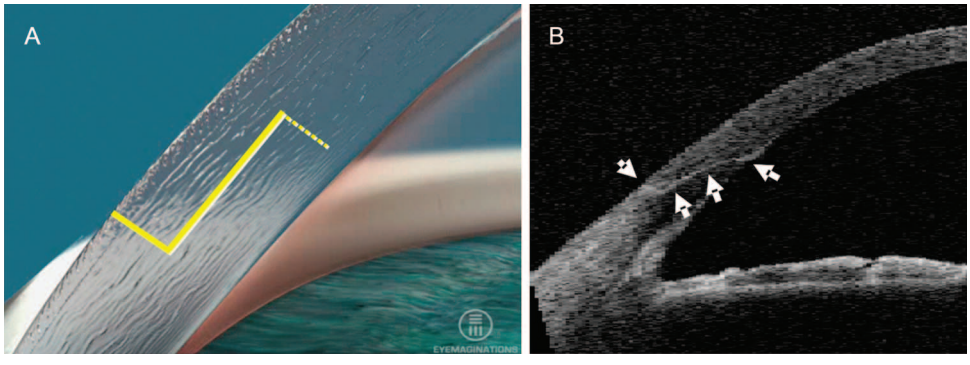

Fig. 5. Details of the corneal incision. (**A**) Diagram of the planned corneal incision. Dashed line shows a segment that will be cut later by a blade in the operating room. (**B**) OCT image of the cataract incision next day after surgery. Arrows, white line indicating incision.

The resulting images of the patterns in the patient's eye, as seen from the surgical microscope after the patient was in the operating room (Fig. 6A), showed the round edge of the capsulotomy and the lens fragmentation patterns. The circular segment of the capsule was removed with forceps, by a circular movement, similar to a capsulorhexis. Such removal was safer than just pulling it out, in case there are any remaining bridges connecting the dissected disk with the capsular bag. The extracted lens capsule was stained, flattened between glass slides, and imaged, and its size was measured with light microscopy. The imaging system was calibrated with an NIST (National Institute of Standards and Technology)–traceable reference reticule.

Representative images of the capsules extracted after laser capsulotomy and conventional manual capsulorhexis are shown in Fig. 7. The size of the extracted capsular disk was determined as follows: The sample was measured along its x and y axes, rotated 45°, and measured again. These values were averaged to yield the average capsule diameter. Deviation from intended size in manual capsulorhexis was −282 ± 305 μm (n = 30), whereas with laser capsulotomy it was 27 ± 25 μm (n = 29) (P < 0.001). We measured the circularity of the extracted capsule as a normalized ratio of its area to the area of a disk with the diameter equal to the greatest linear dimension of the sample. For an ideal circle, this ratio is equal to 1. For manual capsulorhexis, it was 0.77 ± 0.15 (n = 22), whereas for

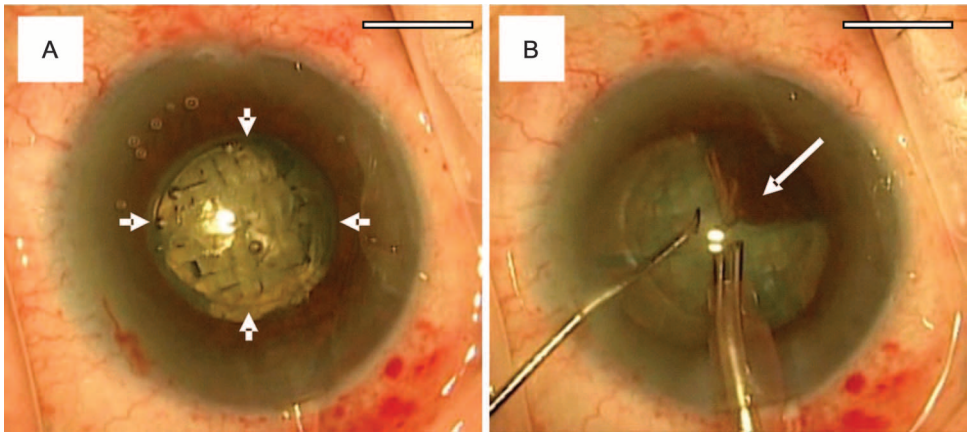

Fig. 6. Images obtained during surgery showing capsule and lens removal. (**A**) View of the eye through the operating microscope after the capsule removal. Arrows, boundaries of the capsulotomy. (**B**) Same eye as in (A) after emulsification and removal of one quadrant of the lens (arrow). Scale bars, 3 mm.

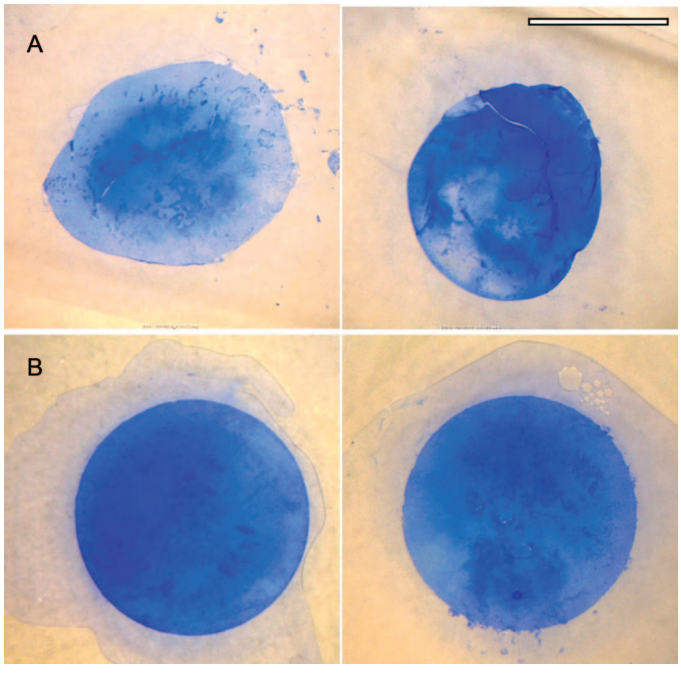

Fig. 7. Precision and reproducibility of lens capsule extraction. (**A** and **B**) Representative examples of the human lens capsule extracted after (A) manual capsulorhexis and (B) laser capsulotomy. Scale bar, 3 mm.

laser capsulotomy, it was 0.95 ± 0.04 (n = 29) (P < 0.001). Right after the removal of the capsular disk, the capsulotomy opening was measured with an intraocular ruler forceps. Its size was ~0.4 mm larger than the resected capsular disk. We surmised that this enlargement was due to stretching and retraction of the lens capsule after capsulotomy.

After the capsular disk was removed, an ultrasonic phacoemulsification instrument was inserted into the anterior chamber together with a chopper, which facilitated splitting the lens into four quadrants along the cross-segmentation pattern. Without effort, the cuts propagated all the way to the bottom of the lens, separating it into four quadrants. The quadrants were then easily aspirated with minimal or no ultrasound energy (Fig. 6B). Our approach resulted in decrease of the perceived hardness of the nuclear sclerotic cataract (as estimated by the surgeon) from grade 4 to grade 2, making its emulsification much easier and faster. The cumulative dispersed energy of the phacoemulsification was reduced in laser-treated eyes on average by 39% (n = 29) relative to their patient-matched manual control eye (n = 30). After extraction of the crystalline lens and insertion of the IOL, the diameter of the capsular opening returned to within 50 μm of the width of the initial laser incision.

The resulting appearance of the capsulotomy edge in a slit lamp examination the next day after surgery is shown in Fig. 8A. The central position and proper sizing of the capsular opening resulted in a symmetric 0.5-mm overlap of the lens capsular bag to the edge of the 6-mm-diameter IOLs. Histological analysis and scanning electron microscopy (SEM) of the capsule extracted during surgery demonstrated a sharp and continuous edge without nicks or radial tears (Fig. 8, B and C). Microgrooves produced by the laser pulses could be seen on the SEM image.

Fifty patients underwent cataract surgery with the femtosecond laser system, selected by the criteria listed in Materials and Methods. Of these, 30 patients were treated as a case-controlled study, with random assignment of one eye to the femtosecond laser group, whereas the other eye was used as matched control for conventional manual cataract surgery. About 80% of the patients exhibited small petechial conjunctival hemorrhages and vasodilatation in a ring pattern corresponding to the suction skirt, similar to that observed after LASIK corneal flap creation with a femtosecond laser. As in LASIK refractive surgery, these conjunctival findings resolved within 7 days. Thirty-eight percent of patients in the laser group and 70% in the control group showed mild corneal edema after surgery, which was within the conventional postoperative limits for phacoemulsification. Corneal edema was not associated with the laser itself. Corneas remained clear after the laser treatment and during the cataract surgery. In cases when relaxing incisions were produced without cataract surgery, there was no corneal edema. No retinal damage or other laser-related adverse events were observed in any of the laser-treated patients.

In the case-controlled group of patients, we measured improvement in the best-corrected visual acuity (BCVA) in the laser-treated (n = 29) and in the control (n = 30) eyes. In the laser group, the mean gain in visual acuity was 4.3 ± 3.8 lines, whereas in the control eyes the mean gain was 3.5 ± 2.1 lines. The difference was not statistically significant (fig. S3). Nevertheless, similarity in the visual outcomes of the laser and manual surgery confirms safety of the laser treatment and lack of side effects on visual function. Evaluation of superiority of the visual outcomes with the laser treatment will require a large comparative clinical trial.

DISCUSSION

An integrated optical system including OCT imaging and a femtosecond laser allowed for exact placement, precise sizing, and shaping of

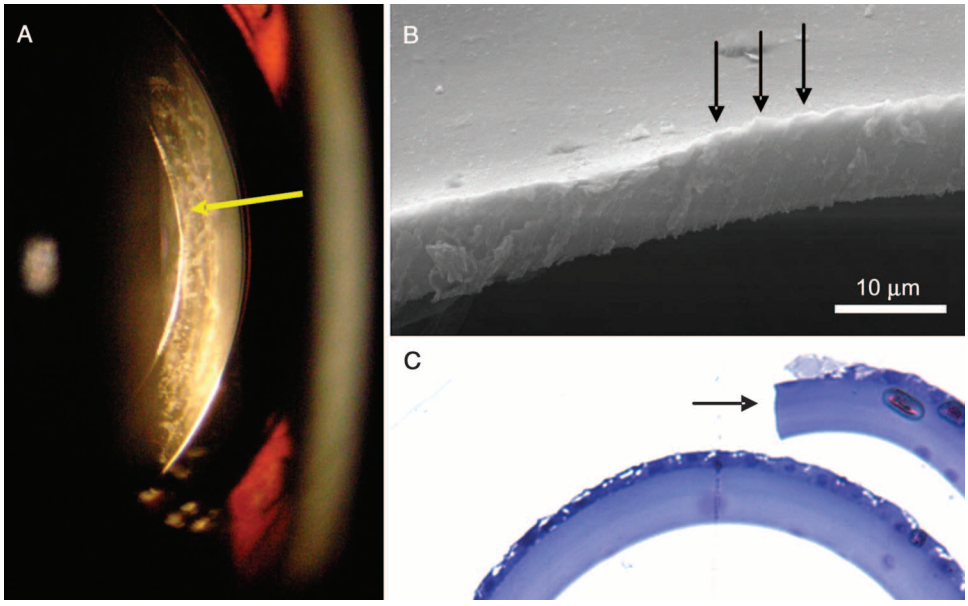

Fig. 8. Images obtained after surgery. (**A**) Slit lamp view of the edge of the capsule 1 day after surgery (arrow). (**B**) Scanning electron micrograph of the edge of the capsule. Note microgrooves produced by each laser pulse (arrows). Scale bar, 10 µm. (**C**) Histology of the lens capsule removed from the eye, stained with toluidine blue. Note a very sharp, clean edge (arrow).

the cutting patterns during surgery to remove cataracts. The continuous sharp-edged capsular cuts improved the strength of the capsule, reducing the risk of its rupture during phacoemulsification and IOL insertion. Lens segmentation and nucleus fragmentation simplified its emulsification, and were especially advantageous with dense cataracts. A multiplanar corneal cut provided for a self-sealing cataract incision.

Automation of portions of cataract surgery facilitated by a femtosecond laser confers a number of benefits for the surgeon and patient (*2*–*11*). A symmetric, well-centered, and properly sized capsulorhexis is critically important in achieving optimal IOL performance, especially for toric, multifocal, and accommodating IOLs. Moreover, the size of the capsulotomy and its construction has a direct relation to effective lens position (*12*). Inaccurate prediction of the effective lens position was identified as the biggest source of error in IOL power calculations (*19*). A difference of 1 mm in lens position can lead to an ~1.25 diopters (D) change in refractive error (*20*–*22*). For toric and multifocal IOLs, the window for error is even smaller: Tilt, decentration, or rotation with these IOLs can cause significant deviations from the desired refractive outcome, in addition to visual aberrations that are difficult to tolerate (*23*, *24*). The effective axial position of the IOL may also vary depending on whether the capsulorhexis completely or incompletely overlaps the optic (lens), thereby affecting accuracy of the IOL power calculation. Most accommodating IOLs should not be implanted if the capsulorhexis is suboptimal. As an example, a dual optic accommodating IOL designed to produce forward movement of the anterior optic during accommodative effort (*25*, *26*) requires a completely overlapping capsulorhexis to prevent partial prolapse of the anterior optic out of the capsular bag. Therefore the precisely sized and centered capsulotomy incisions enabled by this method should improve predictability and control of the IOL placement. Precision in sizing of the capsulotomy with the femtosecond laser was 12 times better than that with manual capsulorhexis: The deviations from the intended size decreased from ±305 to ±25 µm. Accuracy in shaping improved by about a factor of 5: Deviation from round shape decreased from 23 to 5% with the laser.

Another significant advantage of the laser procedure is improved strength of the capsulotomy—by more than a factor of 2, compared to the manual technique—which makes the capsule manipulation during phacoemulsification and IOL insertion safer.

One of the most fundamental differences of this system from the femtosecond lasers currently used in refractive surgery (LASIK flap cutting) is in integration of the surgical laser with OCT imaging. A precise three-dimensional map of the cornea, posterior, and anterior capsule allows for exact positioning of the cutting patterns within the target tissue. Separately obtained OCT before surgery does not reflect the deformations in the eye caused by attachment to the suction ring during the procedure. Intraoperative imaging also allows for precise centration of the capsulotomy and exact positioning of the corneal relaxing incisions. In addition, it allows for exact placement of the multiplanar self-sealing cataract incision that does not penetrate the posterior corneal surface. Lack of penetration into the anterior chamber allows maintenance of the intraocular pressure and performance of this step before introduction of the patient into the sterile operating room.

The difficulty of creating a successful capsulorhexis can be exacerbated by poor capsular visibility, a small pupil, a shallow anterior chamber, weak zonules, a thickened and fibrotic capsule, absence of the red reflex, an intumescent white cataract, or an elastic pediatric anterior capsule. A variety of methods to trace or draw a capsulorhexis have been considered and tested (*27*–*29*). One of these, a high-frequency electrosurgical capsulotomy probe, has been reported to produce thermal damage to the edge of the capsule, thereby decreasing its biomechanical stability (*27*, *28*, *30*). Vitrectorhexis, a mechanized anterior capsulotomy technique, has been associated with an incidence of radial tears as high as 7.7% (*31*). The Fugo blade, a bipolar continuous radio frequency cutter (*29*, *32*), is somewhat bulkier and heavier than a conventional cystotome and requires an extended learning period. A higher percentage of radial tears with this method were found in one clinical study (*31*). Another electrosurgical device, the pulsed electron avalanche knife (PEAK), has been recently introduced for precise cutting of ocular tissues without thermal damage. It produces a sharp and clean-edged capsulotomy, without radial nicks and tears (*33*–*35*). However, it is still a manual procedure, with the associated problems of centration and sizing of the capsulotomy.

An additional advantage of laser-assisted cataract surgery is the reduction of the perceived lens hardness during phacoemulsification, which results from its fragmentation into easily aspiratable pieces. Results of the current initial trial indicated an ~40% reduction in the use of ultrasound energy during phacoemulsification (cumulative dissipated energy). With more experience and development of addi-

tional segmentation patterns, this improvement may increase further. Simplification of the lens emulsification procedure should also help to further reduce the size of the cataract incision, making cataract surgery less invasive (*36*, *37*). It may also allow a decrease in the size of the capsulotomy, an important step toward a lens refilling procedure to restore accommodation (*38*, *39*).

Normal corneal aging and associated opacification did not limit the ability to use laser for cataract surgery. Because near-infrared wavelength of the laser (1030 nm) is scattered much less than visible light (400 to 700 nm), it is unlikely that mild corneal opacification will preclude the use of lasers in cataract surgery. However, significant scarring in the central cornea may be a limiting factor. The exact extent of corneal and lens opacification that will affect laser surgery remains to be determined experimentally.

Femtosecond lasers in the near-infrared part of the spectrum have been successfully used for dissection of the corneal flap in LASIK. However, three-dimensional segmentation of the crystalline lens for cataract surgery requires different laser parameters. Because of the much larger focal depth required, a numerical aperture of the laser focusing system is accordingly reduced. The focal beam diameter is therefore correspondingly increased compared to that in corneal surgery. This results in higher threshold energy necessary for dielectric breakdown, which in turn leads to limitations on the repetition rate to maintain the average retinal exposure with the thermal safety limits.

Two mechanisms of retinal damage should be considered when operating with a pulsed laser at a high repetition rate. The first is the potential for thermomechanical damage to retinal pigment epithelium cells by rapid overheating of the melanosomes with high-energy ultrashort pulses. Typical threshold energy fluence for such phenomenon is 100 mJ/cm^2 (*40*). In our focusing system, the retinal spot size is not smaller than 2.4 mm in diameter, and pulse energy does not exceed 10 μJ; therefore, the retinal energy fluence levels do not exceed 0.2 mJ/cm^2, or 0.2% of the damage threshold.

The second limitation is the average heating of the retina by the scanning beam. Following the American National Standards Institute (ANSI) ocular laser safety standards (*41*, *42*), the described laser system is limited in retinal irradiance as a function of the irradiation duration t, as follows: $9.4t^{-0.25}$ (W/cm^2) (*41*). The system parameters, as described above, were set to not exceed these limits at maximum settings, even when assuming that all of the laser energy is transmitted to the retina. This is a conservative estimate because plasma formation in the focal point provides some blocking of the radiation, and water absorption in the eye at 1030-nm wavelength provides attenuation by a factor of 2. Additionally, bubble layers formed during the laser procedure further scatter the beam, providing increased retinal safety as the pattern progresses.

A typical pattern for capsulotomy (Fig. 3C) is a cylinder of 5 mm in diameter and 400 μm in depth. With pulse spacing of 5 μm in the plane of the cylinder and 10 μm in depth, this pattern is composed of 3141 × 40 or 125,640 spots. At a repetition rate of 50 kHz, application of such a pattern takes ~2.5 s. Similarly, a cross-pattern of 7 mm in width and 3 mm in depth, with a lateral spot separation of 10 μm and depth separation of 20 μm, includes ~210,000 spots and requires 4.2 s. A nucleus fragmentation pattern, such as one shown in Fig. 2C, contains ~360,000 spots and can be delivered in ~7.2 s.

In conclusion, an integrated system including OCT imaging and a femtosecond laser with optics and software optimized for pattern cutting can provide multiple benefits for cataract surgery. It allows for exact placement of the cutting patterns determined by both preoperative and intraoperative imaging. The femtosecond laser produces continuous sharp-edged capsular cuts with reduced likelihood of radial nicks or tears, or zonular dehiscence. Improved strength of the capsule after laser capsulotomy could reduce the risk of its rupture during phacoemulsification and IOL insertion. Lens segmentation and nucleus fragmentation simplify its emulsification, especially with dense cataracts. In addition, the multiplanar self-sealing cataract incision and exact placement of the limbal relaxing incisions have the potential to bring cataract surgery to the precision and reproducibility previously attainable only in refractive laser surgery.

MATERIALS AND METHODS

Porcine eyes were obtained from Animal Technologies Inc. and shipped on ice overnight after enucleation. Phakic human donor eyes deemed unsuitable for use for corneal transplant surgery were received from the Lions Eye Bank (Miami, FL) and San Diego Eye Bank (San Diego, CA).

Six Dutch belted rabbits (weight, 1.5 to 2.5 kg) were used in accordance with the Association for Research in Vision and Ophthalmology Resolution on the Use of Animals in Ophthalmic and Vision Research, with approval from the Stanford Research Institute Animal Institutional Review Board (IRB). Ketamine hydrochloride (35 mg/kg), xylazine (5 mg/kg), and glycopyrrolate (0.01 mg/kg) were used for anesthesia. Pupil dilation was achieved by one drop each of 1% tropicamide and 2.5% phenylephrine hydrochloride, and 0.5% topical tetracaine hydrochloride was used for local anesthesia. Both eyes of each rabbit were treated and analyzed with fluorescein angiography and fundus photos within 1 hour after irradiation. For fluorescein angiography, 0.3 ml of 10% fluorescite (Alcon Laboratories) was slowly injected over 10 s into the marginal ear vein as described previously. Fundus photographs and angiography were taken with a Topcon TRC 50× fundus camera (Topcon). Photographs were taken starting a few seconds after the injection and thereafter every 20 s for 5 min. For histology, rabbits were killed 1 hour after treatment with a lethal dose of Beuthanasia (150 mg/kg, intravenously) injected into the marginal ear vein.

Patient selection

To be enrolled in the study, patients between the ages of 50 and 80 years old with grade 1 to 4 nuclear sclerotic cataracts were required to demonstrate an ability to understand the informed consent document and to comply with the treatment and follow-up schedule. Additional criteria included the following: ETDRS (Early Treatment Diabetic Retinopathy Study) visual acuity in the range of 20/30 to 20/80; pupil dilation diameter of no less than 7 mm; ability to fixate; and an axial length of 22 to 26 mm. Patients' age range in the study was from 55 to 80 years, with an average of 70 ± 6 (mean ± SD) years, with 60% females and 40% males. The eyes were randomly assigned to laser or standard cataract surgery. The full range of lens hardness inclusion criteria (grade 1 to 4) was covered, with 50% of patients having LOCS (Lens Opacities Classification System) grade 3 cataract.

Exclusion criteria were as follows: pregnancy or intention to become pregnant; enrollment in another drug or device study within the last 3 months; and history of ocular trauma or coexisting ocular disease affecting vision or ocular surgery, with the exception of cataract surgery. Patients were also excluded if the anterior chamber depth was <2.5 mm or corneal astigmatism was greater than 5 D.

IRB protocol for laser-assisted cataract surgery was approved by the Dominican Republic Independent Review Board (Canabios, Santo Domingo, Dominican Republic). Surgeries were performed in the Laser Centro (Santo Domingo, Dominican Republic).

Sample preparations for histology, SEM, and light microscopy

Extracted human lens capsules were flattened between glass slides and stained with 0.5% trypan blue, and size and shape were measured under a digital light microscope, as described above. For histology, the viscoelastic and remaining lens cortex was removed from the extracted capsule with saline and fixed in 1% paraformaldehyde overnight at room temperature.

For SEM, tissue was fixed in 2.5% glutaraldehyde in sodium cacodylate buffer (pH 7.4), postfixed in 1% osmium tetroxide, dehydrated in a series of methanols, and critical point–dried. The samples were plasma coated with gold-palladium and evaluated with a scanning electron microscope.

For histology, the rabbit eyes were postfixed in osmium tetroxide, dehydrated with a graded series of ethanol, processed with propylene oxide, embedded in an epoxy resin, and sectioned into 1-μm-thick sections. Samples were stained with toluidine blue and examined by light microscopy.

Measurements of the capsulotomy size and centration

Measurements of size and shape of the extracted lens capsular disk was performed by the digital light microscopy of the stained samples, calibrated with an NIST-traceable reference standard. The size of the extracted capsular disk was measured as follows: The sample was aligned with its maximum width along the x axis, and its size was calculated as an average of four measurements (the width along the x and y axes, and the width along the axes rotated by 45°). Circularity of the extracted capsule was measured as a ratio of the sample area to the area of a disk with diameter corresponding to the greatest linear dimension of the sample. For an ideal circle, this ratio is equal to 1.

One cross-sectional measurement of the capsulotomy opening was taken during surgery, right after the capsular disk removal, with a Seibel Rhexis ruler (MicroSurgical Technology). One week and 1 month after surgery, patients underwent a dilated eye exam including slit lamp anterior chamber photography. The size and centration of the capsulotomy relative to the dilated pupil were analyzed on the basis of the digital images. Scaling was performed by comparison to the known size of the patient's IOL optic.

SUPPLEMENTARY MATERIAL

www.sciencetranslationalmedicine.org/cgi/content/full/2/58/58ra85/DC1

Fig. S1. Fluorescein angiography of the rabbit eye (A) before and (B) 1 hour after the laser irradiation of the fundus.

Fig. S2. Simplified diagram of the system, including the imaging (OCT) and the treatment (femtosecond laser) modules.

Fig. S3. Changes in the best-corrected visual acuity (BCVA) 1 month after the laser (n = 29) and manual control (n = 30) cataract surgery.

Video 1. Laser capsulotomy and removal of the capsular disk.

Video 2. Laser segmentation and phacoemulsification of the crystalline lens.

REFERENCES AND NOTES

1. *Age-Related Eye Disease Study* (National Eye Institute, NIH, Bethesda, MD, 2010).
2. T. Neuhann, Theory and surgical technique of capsulorhexis. *Klin. Monbl. Augenheilkd.* **190**, 542–545 (1987).
3. H. V. Gimbel, T. Neuhann, Development, advantages, and methods of the continuous circular capsulorhexis technique. *J. Cataract Refract. Surg.* **16**, 31–37 (1990).
4. E. I. Assia, D. J. Apple, J. C. Tsai, E. S. Lim, The elastic properties of the lens capsule in capsulorhexis. *Am. J. Ophthalmol.* **111**, 628–632 (1991).
5. S. Krag, K. Thim, L. Corydon, Strength of the lens capsule during hydroexpression of the nucleus. *J. Cataract Refract. Surg.* **19**, 205–208 (1993).
6. Q. Peng, N. Visessook, D. J. Apple, S. K. Pandey, L. Werner, M. Escobar-Gomez, R. Schoderbek, K. D. Solomon, A. Guindi, Surgical prevention of posterior capsule opacification. Part 3: Intraocular lens optic barrier effect as a second line of defense. *J. Cataract Refract. Surg.* **26**, 198–213 (2000).
7. D. Wasserman, D. J. Apple, V. E. Castaneda, J. C. Tsai, R. C. Morgan, E. I. Assia, Anterior capsular tears and loop fixation of posterior chamber intraocular lenses. *Ophthalmology* **98**, 425–431 (1991).
8. J. Ram, D. J. Apple, Q. Peng, N. Visessook, G. U. Auffarth, R. J. Schoderbek Jr., E. L. Ready, Update on fixation of rigid and foldable posterior chamber intraocular lenses. Part I: Elimination of fixation-induced decentration to achieve precise optical correction and visual rehabilitation. *Ophthalmology* **106**, 883–890 (1999).
9. E. J. Hollick, D. J. Spalton, W. R. Meacock, The effect of capsulorhexis size on posterior capsular opacification: One-year results of a randomized prospective trial. *Am. J. Ophthalmol.* **128**, 271–279 (1999).
10. E. I. Assia, D. J. Apple, J. C. Tsai, R. C. Morgan, Mechanism of radial tear formation and extension after anterior capsulectomy. *Ophthalmology* **98**, 432–437 (1991).
11. M. K. Aasuri, V. B. Kompella, A. B. Majji, Risk factors for and management of dropped nucleus during phacoemulsification. *J. Cataract Refract. Surg.* **27**, 1428–1432 (2001).
12. O. Cekiç, C. Batman, The relationship between capsulorhexis size and anterior chamber depth relation. *Ophthalmic Surg. Lasers* **30**, 185–190 (1999).
13. I. J. Dooley, P. D. O'Brien, Subjective difficulty of each stage of phacoemulsification cataract surgery performed by basic surgical trainees. *J. Cataract Refract. Surg.* **32**, 604–608 (2006).
14. P. Ernest, M. Rhem, M. McDermott, K. Lavery, A. Sensoli, Phacoemulsification conditions resulting in thermal wound injury. *J. Cataract Refract. Surg.* **27**, 1829–1839 (2001).
15. M. A. Sarayba, M. Taban, T. S. Ignacio, A. Behrens, P. J. McDonnell, Inflow of ocular surface fluid through clear corneal cataract incisions: A laboratory model. *Am. J. Ophthalmol.* **138**, 206–210 (2004).
16. P. J. McDonnell, M. Taban, M. Sarayba, B. Rao, J. Zhang, R. Schiffman, Z. Chen, Dynamic morphology of clear corneal cataract incisions. *Ophthalmology* **110**, 2342–2348 (2003).
17. J. H. Talamo, J. Meltzer, J. Gardner, Reproducibility of flap thickness with IntraLase FS and Moria LSK-1 and M2 microkeratomes. *J. Refract. Surg.* **22**, 556–561 (2006).
18. K. G. Carrasquillo, J. Rand, J. H. Talamo, Intacs for keratoconus and post-LASIK ectasia: Mechanical versus femtosecond laser-assisted channel creation. *Cornea* **26**, 956–962 (2007).
19. S. Norrby, Sources of error in intraocular lens power calculation. *J. Cataract Refract. Surg.* **34**, 368–376 (2008).
20. D. R. Sanders, R. W. Higginbotham, I. E. Opatowsky, J. Confino, Hyperopic shift in refraction associated with implantation of the single-piece Collamer intraocular lens. *J. Cataract Refract. Surg.* **32**, 2110–2112 (2006).
21. V. Lakshminarayanan, J. M. Enoch, T. Raasch, B. Crawford, R. W. Nygaard, Refractive changes induced by intraocular lens tilt and longitudinal displacement. *Arch. Ophthalmol.* **104**, 90–92 (1986).
22. P. Erickson, Effects of intraocular lens position errors on postoperative refractive error. *J. Cataract Refract. Surg.* **16**, 305–311 (1990).
23. J. S. Wolffsohn, P. J. Buckhurst, Objective analysis of toric intraocular lens rotation and centration. *J. Cataract Refract. Surg.* **36**, 778–782 (2010).
24. T. Walkow, N. Anders, D. T. Pham, J. Wollensak, Causes of severe decentration and subluxation of intraocular lenses. *Graefes Arch. Clin. Exp. Ophthalmol.* **236**, 9–12 (1998).
25. S. D. McLeod, L. G. Vargas, V. Portney, A. Ting, Synchrony dual-optic accommodating intraocular lens. Part 1: Optical and biomechanical principles and design considerations. *J. Cataract Refract. Surg.* **33**, 37–46 (2007).
26. I. L. Ossma, A. Galvis, L. G. Vargas, M. J. Trager, M. R. Vagefi, S. D. McLeod, Synchrony dual-optic accommodating intraocular lens. Part 2: Pilot clinical evaluation. *J. Cataract Refract. Surg.* **33**, 47–52 (2007).
27. J. E. Morgan, R. B. Ellingham, R. D. Young, G. J. Trmal, The mechanical properties of the human lens capsule following capsulorhexis or radiofrequency diathermy capsulotomy. *Arch. Ophthalmol.* **114**, 1110–1115 (1996).
28. S. Krag, K. Thim, L. Corydon, Diathermic capsulotomy versus capsulorhexis: A biomechanical study. *J. Cataract Refract. Surg.* **23**, 86–90 (1997).
29. D. Singh, Use of the Fugo blade in complicated cases. *J. Cataract Refract. Surg.* **28**, 573–574 (2002).
30. A. Kruger, M. Amon, J. Nepp, Intraoperative and postoperative complications of high-frequency capsulotomy and continuous curvilinear capsulorhexis. *J. Cataract Refract. Surg.* **23**, 429–432 (1997).

31. M. E. Wilson Jr., Anterior lens capsule management in pediatric cataract surgery. *Trans. Am. Ophthalmol. Soc.* **102**, 391–422 (2004).
32. A. M. Izak, L. Werner, S. K. Pandey, D. J. Apple, M. G. J. Izak, Analysis of the capsule edge after Fugo plasma blade capsulotomy, continuous curvilinear capsulorhexis, and can-opener capsulotomy. *J. Cataract Refract. Surg.* **30**, 2606–2611 (2004).
33. D. Palanker, H. Nomoto, P. Huie, A. Vankov, D. F. Chang, Anterior capsulotomy with a pulsed-electron avalanche knife. *J. Cataract Refract. Surg.* **36**, 127–132 (2010).
34. S. G. Priglinger, C. Haritoglou, D. Palanker, D. Kook, M. Grueterich, A. Mueller, C. S. Alge, A. Kampik, Pulsed electron avalanche knife for capsulotomy in congenital and mature cataract. *J. Cataract Refract. Surg.* **32**, 1085–1088 (2006).
35. S. G. Priglinger, D. Palanker, C. S. Alge, T. C. Kreutzer, C. Haritoglou, M. Grueterich, A. Kampik, Pulsed electron avalanche knife: New technology for cataract surgery. *Br. J. Ophthalmol.* **91**, 949–954 (2007).
36. J. L. Alio, H. Fine, *Incisions and Maximizing Outcomes in Cataract Surgery* (Springer-Verlag, Berlin, 2009).
37. C. D. Kelman, Intracapsular lens extraction through a small incision. *Am. J. Ophthalmol.* **69**, 277–283 (1970).
38. Y. Nishi, K. Mireskandari, P. Khaw, O. Findl, Lens refilling to restore accommodation. *J. Cataract Refract. Surg.* **35**, 374–382 (2009).
39. S. Norrby, in *Refractive Lens Surgery*, H. Fine, M. Packer, R. S. Hoffman, Eds. (Springer, Berlin, 2005).
40. G. Schuele, M. Rumohr, G. Huettmann, R. Brinkmann, RPE damage thresholds and mechanisms for laser exposure in the microsecond-to-millisecond time regimen. *Invest. Ophthalmol. Vis. Sci.* **46**, 714–719 (2005).
41. F. C. Delori, R. H. Webb, D. H. Sliney; American National Standards Institute, Maximum permissible exposures for ocular safety (ANSI 2000), with emphasis on ophthalmic devices. *J. Opt. Soc. Am. A Opt. Image Sci. Vis.* **24**, 1250–1265 (2007).
42. The Laser Institute of America (2007).

43. **Acknowledgments:** We thank J. Peca (Florida Lions Eye Bank, Miami, FL) for his assistance with tissue procurement and preparation and R. Dalal (Eye Pathology Lab) for her help with histological preparations and photography. **Funding:** Provided in part by OptiMedica Corp. **Author contributions:** D.P. and M.S.B. invented the system, designed and performed in vitro experiments, and helped with data analysis, development of the clinical system, and writing of the manuscript. D.A., M.W., and G.S. built an integrated system with OCT, performed in vitro experiments with porcine and human samples, and associated analysis of the results. D. Andersen, M.W., P.G., D. Angeley, G.S., B.W., and M.S. built the clinical system and participated in clinical tests. N.J.F., B.S., J.B., R.F., J.T., and W.C. are cataract surgeons who performed preclinical and clinical tests of the system, including experimental and control cataract surgeries, and took part in data analysis and writing of the manuscript. **Competing interests:** M.S.B. is on the Board of Directors of and has equity interest in OptiMedica, which manufactures the femtosecond laser cataract system; N.J.F., J.B., J.T., W.C. are on the Medical Advisory Board and have equity interest in OptiMedica, D.P. and R.F. are paid consultants for OptiMedica. The remaining authors are employees of OptiMedica. OptiMedica has filed patents on the technology described in the paper. US Patent Publications: 60/643056; 11/328970; 12/048182, 12/048185, 12/048186, 12/510148, 12/702242, 12/703687, 12/703689; 61/289837, 61/293357, 61/297624, 61/302437. **Accession numbers:** The clinical trial is registered on ClinicalTrials.gov (NCT00922571 and NCT01069172).

Submitted 21 May 2010
Accepted 29 October 2010
Published 17 November 2010
10.1126/scitranslmed.3001305

Citation: D. V. Palanker, M. S. Blumenkranz, D. Andersen, M. Wiltberger, G. Marcellino, P. Gooding, D. Angeley, G. Schuele, B. Woodley, M. Simoneau, N. J. Friedman, B. Seibel, J. Batlle, R. Feliz, J. Talamo, W. Culbertson, Femtosecond laser–assisted cataract surgery with integrated optical coherence tomography. *Sci. Transl. Med.* **2**, 58ra85 (2010).

Science Translational Medicine
AAAS

Femtosecond Laser–Assisted Cataract Surgery with Integrated Optical Coherence Tomography

Daniel V. Palanker, *et al.*

Sci Transl Med **2**, 58ra85 (2010);
DOI: 10.1126/scitranslmed.3001305